HHS Public Access

Author manuscript

Resour Conserv Recycl. Author manuscript; available in PMC 2023 January 01.

Published in final edited form as:

Resour Conserv Recycl. 2022 January ; 176: . doi:10.1016/j.resconrec.2021.105911.

Towards sustainable additive manufacturing: The need for awareness of particle and vapor releases during polymer recycling, making filament, and fused filament fabrication 3-D printing

Aleksandr B. Stefaniak[a,*], **Lauren N. Bowers**[a], **Gabe Cottrell**[b], **Ergin Erdem**[b], **Alycia K. Knepp**[a], **Stephen B. Martin Jr.**[a], **Jack Pretty**[c], **Matthew G. Duling**[a], **Elizabeth D. Arnold**[a], **Zachary Wilson**[b], **Benjamin Krider**[b], **Alyson R. Fortner**[a], **Ryan F. LeBouf**[a], **M. Abbas Virji**[a], **Arif Sirinterlikci**[b]

[a]National Institute for Occupational Safety and Health, Respiratory Health Division, Morgantown, WV, 26505, United States

[b]Robert Morris University, School of Engineering, Mathematics, and Science, Moon Township, PA, 15108, United States

[c]National Institute for Occupational Safety and Health, Health Effects Laboratory Division, Cincinnati, OH, 45213, United States

Abstract

Fused filament fabrication three-dimensional (FFF 3-D) printing is thought to be environmentally sustainable; however, significant amounts of waste can be generated from this technology. One way to improve its sustainability is via distributed recycling of plastics in homes, schools, and libraries to create feedstock filament for printing. Risks from exposures incurred during recycling and reuse of plastics has not been incorporated into life cycle assessments. This study characterized contaminant releases from virgin (unextruded) and recycled plastics from filament production through FFF 3-D printing. Waste polylactic acid (PLA) and acrylonitrile butadiene styrene (ABS) plastics were recycled to create filament; virgin PLA, ABS, high and low density polyethylenes, high impact polystyrene, and polypropylene pellets were also extruded

[*]Corresponding author at: National Institute for Occupational Safety and Health, 1095 Willowdale Road, Morgantown, WV, 26505, United States. AStefaniak@cdc.gov (A.B. Stefaniak).

Author contributions

Aleksandr B. Stefaniak: Conceptualization, Formal analysis, Data curation, Investigation, Writing – Original draft, Supervision, Funding acquisition; **Lauren N. Bowers:** Conceptualization, Formal analysis, Data curation, Investigation, Writing – Review & Editing, Visualization; **Gabe Cottrell:** Investigation, Resources; **Ergin Erdem:** Investigation, Resources; **Alycia K. Knepp:** Conceptualization, Formal analysis, Data curation, Investigation, Writing – Review & Editing, Visualization; **Stephen B. Martin, Jr.:** Validation, Investigation; **Jack Pretty:** Methodology, Validation, Writing – Review & Editing; **Matthew G. Duling:** Investigation; **Elizabeth D. Arnold:** Formal analysis, Data curation, Writing – Review & Editing, Visualization; **Zack Wilson:** Investigation; **Benjamin Krider:** Investigation; **Alyson R. Fortner:** Investigation; **Ryan F. LeBouf:** Methodology, Validation, Writing – Review & Editing; **M. Abbas Virji:** Formal analysis, Writing – Review & Editing, Visualization; **Arif Sirinterlikci:** Investigation, Resources, Writing – Review & Editing.

Declaration of Competing Interest

The authors declare that they have no known competing financial interests or personal relationships that could have appeared to influence the work reported in this paper.

Supplementary materials

Supplementary material associated with this article can be found, in the online version, at doi:10.1016/j.resconrec.2021.105911.

into filament. The release of particles and chemicals into school classrooms was evaluated using standard industrial hygiene methodologies. All tasks released particles that contained hazardous metals (e.g., manganese) and with size capable of depositing in the gas exchange region of the lung, i.e., granulation of waste PLA and ABS (667 to 714 nm) and filament making (608 to 711 nm) and FFF 3-D printing (616 to 731 nm) with waste and virgin plastics. All tasks released vapors, including respiratory irritants and potential carcinogens (benzene and formaldehyde), mucus membrane irritants (acetone, xylenes, ethylbenzene, and methyl methacrylate), and asthmagens (styrene, multiple carbonyl compounds). These data are useful for incorporating risks of exposure to hazardous contaminants in future life cycle evaluations to demonstrate the sustainability and circular economy potential of FFF 3-D printing in distributed spaces.

Keywords

3-D printing; Plastics; Circular economy; Schools; Libraries; Health

1. Introduction

Material extrusion (ME) is a type of additive manufacturing process that selectively dispenses feedstock through a nozzle to build a part layer-by-layer (ISO/ASTM, 2015). One variation of ME is fused filament fabrication (FFF) 3-D printing, in which thermoplastic filament is heated in an extruder nozzle to above its glass transition temperature and dispensed onto a build platform, layer-by-layer, based on a computer design file to build a part. During operation, FFF 3-D printers release particles (often with diameter < 100 nm) and volatile organic compounds (VOCs), which result in exposures to workers (Du Preez et al., 2018; Stefaniak et al., 2019).

Additive manufacturing processes add feedstock material to create a part. These processes are generally thought to be more environmentally sustainable than traditional (*e.g.*, subtractive) manufacturing techniques by making more efficient use of raw materials and producing less waste (Huang et al., 2013). In practice, significant amounts of plastic waste can be generated from FFF 3-D printing (*e.g.*, parts that do not meet build criteria, unused feedstock, and printed parts that have reached the end of their useful service life), which has raised questions on sustainability for widespread adoption of this technology (Hunt et al., 2015; Pakkanen et al., 2017; Song et al., 2019; Song and Telenko, 2016, 2017; Zhao et al., 2018; Zhong and Pearce, 2018). Access to 3-D printers is a major determinant of waste generation rates (Song et al., 2019). With the adoption of additive manufacturing rising (Thomas, 2016), FFF 3-D printing could significantly contribute to waste streams.

One means to improve the sustainability of FFF 3-D printing is via recycling of plastics (Baechler et al., 2013; Hunt et al., 2015; Kreiger et al., 2014; Mikula et al., 2021; Peeters et al., 2019; Suárez and Domínguez, 2020; Zhong and Pearce, 2018). Centralized recycling of plastics by municipal waste management can be uneconomical and energy intensive (Baechler et al., 2013; Kreiger et al., 2014). As such, some researchers propose recycling waste polymers at distributed sites (homes, schools, libraries, etc.) to create feedstock filament for FFF 3-D printers (Baechler et al., 2013; Kreiger et al., 2014; Song et al.,

2019; Zhong and Pearce, 2018). Commercial extruders for converting polymers into FFF 3-D printer filament are available on the consumer market (Kreiger et al., 2014). Polymer material, in the form of pellets (usually virgin polymer) or shredded granules (waste polymer), is fed into the machine, heated, and extruded through an orifice to produce filament. Both FFF 3-D printers and commercial filament extruders heat polymer and dispense it via an orifice or nozzle. Hence, Byrley et al. hypothesized that filament extruders would also release particles and VOCs. They evaluated emissions in an environmental test chamber while extruding virgin acrylonitrile butadiene styrene (ABS) and polylactic acid (PLA) plastics into filaments; particle number concentrations were higher during extrusion of ABS compared with PLA. During extrusion of ABS into filament, ethylbenzene and styrene were quantified in chamber air and during extrusion of PLA into filament, benzene, toluene, and styrene were quantified in chamber air (Byrley et al., 2019).

If distributed polymer recycling is performed in an office, home, library, school, or other space that lacks engineering controls such as local exhaust ventilation, particles and VOCs released into air might not be removed sufficiently to prevent exposures to extruder operators. Several investigators have evaluated contaminant concentrations adjacent to an additive manufacturing process, *i.e.*, the near field (NF), and at a distance from the process, *i.e.*, the far field (FF). Some studies indicated that contaminant concentrations were similar or higher in the FF compared with the NF, which suggested that bystanders to a process can also be exposed, though results are conflicting (Bau et al., 2020; Bharti and Singh, 2017; Chan et al., 2020; Lewinski et al., 2019; Zhou et al., 2015).

To improve understanding of the sustainability of FFF 3-D printing, future life cycle assessments should include potential risks from exposures incurred during distributed recycling of waste plastics into feedstock filament and printing parts. To our knowledge, there currently is no data published (in the English language) that provides insights on emissions throughout the entire process of plastics recycling (granulation, filament extrusion) to production of a final part (FFF 3-D printing) for a range of plastics encountered in FFF 3-D printing to use in life cycle assessments. Hence, the objectives of this investigation were to: (1) evaluate contaminant releases during the recycling of waste ABS and PLA into feedstock filament; (2) evaluate contaminant releases during the extrusion into feedstock filament of virgin ABS and PLA pellets as well as four other types of virgin plastic pellets; (3) compare contaminant releases during filament extrusion to releases during FFF 3-D printing for all polymers; and (4) evaluate NF and FF contaminant levels for all polymers. To achieve these four objectives, a suite of complementary and confirmatory real-time particle and gas monitors and time-integrated sampling methods were incorporated into the study design, which was conducted in a real-world setting. Real-time instruments provided information on acute changes in particle number concentration and size (from nanoscale to micronscale) and gas concentration levels, while time-integrated sampling approaches gave quantitative information on specific contaminants of health concern. Given this study design, results are presented herein for a wide range of plastics that are commonly used for FFF 3-D printing and/or that are high volume plastics that usually end up in landfill, so they are being evaluated as filament for FFF 3-D printing. These data cover a breadth of types of plastic and are useful for incorporating exposure risks in future life cycle analyses of FFF 3-D printing (Bours et al., 2017).

2. Materials and methods

A distributed recycling process was used to convert waste ABS and PLA plastic parts into FFF 3-D printer filaments. The source of waste plastics was FFF 3-D printed parts from student design projects that were discarded because they did not meet build criteria or were no longer wanted. These parts were originally printed using filament from multiple manufacturers, so it was impossible to discern which waste parts were made with which manufacturer's filament. As such, the recycled ABS and PLA filaments represent multiple manufacturers, which is typical of a real-world distributed recycling setting. In reality, for distributed recycling, considerable effort would be needed to segregate waste plastic by manufacturer and specific model. Such segregation might be possible for self-generated 3-D printing waste, but even then, the user must know which printed parts were made with which variations of a polymer (e.g., ABS or ABS with flame retardants) and track the part throughout its lifespan, then sort and store them accordingly to recycle. Users who recycle plastics from food packaging and other domestic sources will, at most, know the type of polymer based on its resin identification code, but it will be impossible for them to know the specific additives in these plastics. Therefore, all recycled polymers are expected to have heterogeneous pedigree so the resultant 3-D printing filament will have properties (mechanical and rheological) and emissions that reflect the unique properties of the source plastics.

The waste recycling process encompassed two steps, granulation of waste material and extrusion of these granules into filament (Supplemental Figure S1). Virgin plastics were purchased in pellet form so only the extrusion step was necessary to create filament. Herein, the term virgin refers to polymers that were not previously extruded on a FFF 3-D printer, as opposed to unmodified base polymer, because all virgin polymer pellets contained white colorants. Subsequently, all filaments were used to print the same part using the same FFF 3-D printer.

Six types of polymers were evaluated in this study: ABS, PLA, high density polyethylene (HDPE), low density polyethylene (LDPE), polypropylene (PP), and high impact polystyrene (HIPS). For ABS and PLA, both a recycled and a virgin polymer filament were created; all other polymers made into filament were virgin polymers. Filaments extruded from waste polymers are herein referred to as recycled ABS (rABS) and PLA (rPLA). The designation virgin (v) is used only for the ABS and PLA polymers when necessary to differentiate them from the recycled polymers. ABS, PLA, HDPE, PP, and HIPS were chosen because they represent a broad array of common polymers used in FFF 3-D printing (Wu et al., 2020) and therefore are polymers that will be encountered when recycling 3-D printer waste (Mikula et al., 2021). LDPE is less commonly used for FFF 3-D printing (Wu et al., 2020); however, globally it is a high-production volume plastic that often ends up in landfill, so there is active research into recycling LDPE into filament (Cruz Sanchez et al., 2020; Mikula et al., 2021). It should be noted that each of these polymers has unique properties (e.g., stiffness, inertness, dimensional stability) that dictate their utility for various applications (Wu et al., 2020). Evaluation of a broad range of polymer types, each having unique chemistry, is a strength and novel aspect of the work because it helps to fill the data need on emissions from a range of recyclable plastics for life cycle assessors. For example,

plastics with lower relative emissions might have a more favorable life cycle assessment than plastics that are higher emitters. Future studies should look at variations of the same type of plastic, e.g., ABS is sold with flame retardants and various fillers, as these variations in composition could also influence emissions during recycling.

All recycling and FFF 3-D printing activities were performed in a real-world setting where distributed recycling is performed regularly. A real-world experimental design was deemed a more useful model than a laboratory emissions study given our study objectives. This real-world scenario enabled us to provide data useful for life cycle assessments because it reflected emissions under conditions of actual use, whereas chamber-based emissions testing would suffer from limitations of non-representative size and ventilation air exchange rates (compared with a real-world room) and the absence of real-world variability (e.g., presence of occupants in the room).

2.1. Granulation of waste polymers

Granulation of waste ABS and PLA polymer was performed in a 608 m^3 engineering laboratory with a room air exchange rate (AER) of 4.5/hr, as determined using sulfur hexafluoride (SF_6) tracer gas (ASTM, 2017). SF_6 concentrations were measured using three photoacoustic infrared gas analyzers (Innova, Model 1412, CAI, Orange, CA, USA) positioned at different spatial locations throughout the room. Measurements were performed in duplicate to get an average air exchange rate. Waste plastic was passed through a granulator (Model 611SR, Rapid Systems Inc, Leetsdale, PA) equipped with a 3/16-inch screen twice to ensure that the resulting chip size was sufficiently homogeneous for extrusion into filament. Release of particle and VOC contaminants was monitored in the NF and FF (see Fig. 1).

2.2. Making filament via extrusion

Waste ABS and PLA granules as well as virgin ABS, PLA, HDPE, LDPE, PP, and HIPS pellets were extruded into filament in a 278 m^3 teaching laboratory (AER of 9.3/hr determined by SF_6 decay). The commercial extruder system consisted of an extruder, air path cooler, and filament spooler in series. Virgin HDPE, LDPE, HIPS, and PP polymers were purchased from manufacturer A, virgin ABS and PLA were purchased from manufacturer B. Granulated waste plastic particles or virgin pellets were placed in the extruder hopper, melted, extruded as a softened filament, pulled across the air path cooler to bring back to a hardened state, then wound onto a spool.

The waste ABS and PLA were extruder twice. The first “rough” extrusion was used to identify appropriate extruder conditions (e.g., temperature, spooler take-up speed) and yielded filament with air bubbles from residual moisture in the polymer and some portions with asymmetrical cross-sectional shape. This rough extruded filament was ground into homogeneous particles using a laboratory mill (Model 3383-L10, Thomas Scientific, Swedesboro, NJ). The second, “final” extrusion, used the settings and ground particles from the rough step, and yielded filament with a circular diameter of 2.85 mm (see Supplemental Figure S2). The virgin polymers only required one extrusion (herein referred to as final extrusion) to make 2.85-mm filaments for FFF 3-D printing (see Figure S2). Release of

particle and VOC contaminants was monitored in the NF and in two FF locations designated FF1 and FF2 (see Fig. 1).

2.3. FFF 3-D printing

All filaments were used to print a “dog bone” tensile test part in accordance with ASTM D638 (Mohammed et al., 2019). The rABS, rPLA, and virgin ABS, PLA, HDPE, LDPE, HIPS, and PP filaments were printed using a commercially available FFF 3D printer. Supplemental Table S1 summarizes the FFF 3-D printing parameters for all polymers. For HDPE and HIPS, commercially available glue was used to help adhere the extruded polymer to the build platform. Releases of particle and VOC contaminants were monitored in the NF and up to two FF locations (designated FF1 and FF2 as they were approximately 2 m from the printer – see Fig. 1). Sampling durations for particle- and vapor-phase contaminants were equivalent to the task durations given in the tables (Section 3).

2.4. Particle and VOC measurements

Aerosol released into the rooms was monitored in real-time using an aerodynamic particle sizer (APS, Model 3321, TSI Inc., Shoreview, MN) capable of determining particle number concentration and size (range: 0.5 – 20 μm; 20 second logging interval), an optical particle sizer (OPS, Model 3330, TSI Inc.) capable of determining particle number concentration and size (range: 0.3 – 10 μm; 1 second logging interval), a fast mobility particle sizer (FMPS, Model 3091, TSI Inc.) capable of determining particle number concentration and size (range: 5.6 – 560 nm; 1 second logging interval), and a condensation particle counter (P-Trak, Model 8525, TSI Inc.) to determine particle number concentration (range: 20 – 1000 nm; 1 second logging interval). All instruments were calibrated by their manufacturer and performance verified before use. Real-time total VOCs (TVOC) were monitored using a photoionization detector (PID) with 10.6 eV lamp and 1 second logging interval (Ion Science Inc, Stafford, TX, USA). The PID was calibrated and span checked with isobutylene prior to use. Results were converted to $\mu g/m^3$ as isobutylene equivalents; the instrument limit of detection (LOD) is 1 ppb or 2.3 $\mu g/m^3$.

To quantify specific VOCs, air samples were collected using 450-mL Silonite®-coated evacuated canisters (Model 29-MC450SQT, Entech Instruments Inc., Simi Valley, CA, USA) with flow-controllers followed by analysis of 14 target compounds (acetaldehyde, acetone, benzene, D-limonene, ethanol, ethylbenzene, n-hexane, methyl methacrylate, methylene chloride, styrene, toluene, *α*-pinene, *m,p*-xylene, and *o*-xylene) using gas chromatography-mass spectrometry by National Institute for Occupational Safety and Health (NIOSH) Manual of Analytical Methods (NMAM) 3900 (NIOSH, 2018). Multiple types of samples were collected by drawing air through media using calibrated sampling pumps (AirChek XR5000, SKC Inc., Eighty Four, PA) followed by off-line analysis. Specifically, airborne particles were collected onto mixed cellulose ester (MCE) filters at 3.0 liters per minute (L/min) followed by offline analysis for elements using inductively coupled plasma-optical emission spectrometry in accordance with NMAM 7303 (NIOSH, 2003). Particles were also collected onto quartz fiber filters (QFF, Cat.# 225–401, SKC Inc.) at 3.0 L/min during granulation and extrusion of waste ABS and analyzed for bisphenol A (BPA) using high performance liquid chromatography with ultraviolet detector (HPLC-

UV) in accordance with U.S. Occupational Safety and Health Administration (OSHA) Method 1018 (OSHA, 2013). QFF samples collected during 3-D printing with rABS and vABS were analyzed for BPA by liquid chromatography-mass spectrometry as described previously (Stefaniak et al., 2021a). During FFF 3-D printing only, samples for vapor-phase aldehydes were collected using cartridges that contained silica gel coated with 2,4-dinitrophenylhydrazine (DNPH) (Cat.# 226–119, SKC Inc.) at 1.5 L/min and analyzed by HPLC-UV for formaldehyde in accordance with NMAM 2016 (NIOSH, 2016) or for 10 aldehydes using U.S. Environmental Protection Agency (EPA) EPA Method TO-11A (EPA, 1999). Finally, samples for total (vapor and particle phase) caprolactam were collected using OSHA versatile sampler (OVS-7) tubes that contained a glass fiber filter and XAD-7 adsorbent (Cat.# 226–57, SKC Inc.) at 2.0 L/min and analyzed by HPLC-UV in accordance with OSHA Method PV2012 (OSHA, 1988). Note that no single air monitoring technique for vapors will capture the full breadth of emissions from the six diverse types of polymers evaluated in the current study. Rather, our purpose for the vapor sampling was to monitor for more common chemicals of health concern (respiratory irritants, potential carcinogens, mucus membrane irritants, and asthmagens) that have been documented in FFF 3-D printer emissions from these types of polymers (Stefaniak et al., 2021b), not to characterize all possible emissions from these polymers. As such, it is likely that other vapor emissions from these filaments were not captured in the sampling strategy (Davis et al., 2019; Zhu et al., 2020), some of which could be of health concern.

Background samples were collected prior to each task to measure existing levels of airborne contaminants. Background and task samples were collected at the same locations to eliminate potential bias from spatial variability of airborne contaminants in the rooms. All results presented herein were background corrected. The specific real-time instruments and time-integrated sampling methods were tailored to each polymer and task, therefore, not all types of samples were collected for all polymers as described in the Section 3 text and figures, and Supplemental File. Each combination of task and polymer was monitored once.

2.5. Data analysis

There were no repeat measures so paired t-tests were used to evaluate the null hypotheses that real-time metrics were equal between the NF and FF locations, between the rough and final extrusion steps, and between filament extrusion and FFF 3-D printing. All statistics were computed in JMP (version 13, SAS Institute Inc., Cary, NC) using a significance level of $\alpha = 0.05$. Plots were created using SigmaPlot (version 14.0, Systat Software, Inc., San Jose, CA); the real-time particle and TVOC concentration measurements spanned orders of magnitude, so data were plotted on a Log_{10} scale for easier visualization of results.

3. Results

Previously, we reported effects of printer temperature and filament type on particle and TVOC emission rates for FFF 3-D printing (Stefaniak et al., 2021c). Herein, we report that exposure potential to airborne contaminants varied within and between granulation, filament making, and FFF 3-D printing tasks. The tabulated data for these tasks are given in

Supplemental Tables S2 – S5. Results of all individual paired t-tests are provided in Table S6 and the main findings are summarized below.

3.1. Contaminant release during granulation of waste ABS and PLA polymers

During granulation, average and peak particle number concentrations measured in the NF (APS, OPS, and P-Trak instruments) were approximately equivalent between waste ABS and PLA polymers (Fig. 2). The one exception was for peak number concentration measured using a P-Trak for waste ABS (48,148 #/cm^3), which was 7.5 times higher compared with the peak for waste PLA (6414 #/cm^3). From the APS data, NF geometric mean (GM) aerodynamic particle sizes (geometric standard deviation, GSD) were 714 nm (1.46) and 667 nm (1.31) for waste PLA and ABS, respectively. NF average and peak particle and TVOC concentrations appeared higher for waste PLA compared with the FF location, whereas the opposite pattern was generally observed for waste ABS polymer. When the PLA and ABS data were combined, average and peak particle number and TVOC concentrations were not statistically different between the NF and FF locations (all p-values ≥ 0.19).

As summarized in Supplemental Figure S3, in the NF, low concentrations of benzene (23.1 μg/m^3), toluene (22.2 μg/m^3), *m,p*-xylene (15.1 μg/m^3), and *o*-xylene (11.5 μg/m^3) were quantified during granulation of waste PLA polymer, whereas only acetaldehyde (18.2 μg/m^3) was quantified in the NF during granulation of waste ABS polymer. Manganese (Mn), vanadium (V), and zinc (Zn) were measured in aerosols released in the NF during granulation of waste PLA (0.1, 1.0, and 4.2 μg/m^3, respectively), and iron (Fe; 3.6 μg/m^3) and Zn (6.8 μg/m^3) were aerosolized during granulation of waste ABS polymer. Toluene was measured at similar concentrations (22 μg/m^3), in both the FF and the NF for waste PLA. During granulation of waste ABS, no single VOC was measured in both the FF and NF locations, both Fe and Mn were detected in the NF and FF locations, while concentrations of BPA and caprolactam were non-detectable, *i.e.*, < 1.3 μg/m^3 and < 6.7 μg/m^3, respectfully. Measurable amounts of formaldehyde were detected, but the levels were lower than the background samples.

3.2. Contaminant release during extrusion of recycled and virgin polymers into filaments

In the NF, during rough extrusion of waste PLA, GM particle sizes for waste PLA (APS data) in the NF were 667 nm (rough) and 682 nm (final). From the OPS, which has a lower size cut-off, the calculated GM particle size for waste PLA in the NF was 335 nm (1.03) during final extrusion (an instrument error precluded reporting particle size in the NF during rough extrusion). Average and peak particle number concentrations measurements were highest for the P-Trak instrument; average and peak TVOC concentrations were approximately 1000 and 3500 μg/m^3, respectively (Fig. 3(a)). NF average and peak particle number concentrations and peak TVOC concentration for waste PLA appeared greater during the final extrusion task (Fig. 3(b)) compared with the rough extrusion task. GM particle sizes (APS data) for waste ABS in the NF were 608 nm (rough and final). Corresponding data for rough and final extrusion of waste ABS are shown in Supplemental Figure S4. In the NF, comparison of the rough (Figure S4(a)) and final (Figure S4(b)) extrusion tasks for waste ABS indicated that peak number concentration measured with an APS instrument was two-fold greater during rough extrusion, but peak number concentration

measured with a P-Trak instrument was greater during final extrusion. It is possible that the higher APS (range: 0.5 – 20 μm) peak concentration during rough extrusion was because the waste granules contained moisture, that when heated in the extruder, released water vapor that promoted agglomeration. Most moisture was evaporated during rough extrusion, so the final extrusion yielded smaller particle sizes that were detectable by the P-Trak. In the NF, average and peak TVOC concentrations for waste ABS were approximately equivalent during the rough (Figure S4(a)) and final (Figure S4(b)) extrusion tasks. From paired t-tests, at the NF location, average and peak particle number and TVOC concentrations were not statistically different between the rough and final extrusions steps for the waste polymers (all p-values ≥ 0.35).

At the FF1 location, during rough extrusion of waste PLA (Fig. 3(a)), average and peak particle number concentrations measured using a P-Trak instrument were higher compared with the APS and OPS instruments. GM particles sizes (OPS data) were 322 nm and 333 nm during rough and final extrusion, respectively (an APS instrument error precluded reporting sizes data from that instrument). Further, at the FF1 location, during final extrusion of waste PLA (Fig. 3(b)), average particle number concentration (P-Trak) was 3020 #/cm^3 (peak = 21,354 #/cm^3) and the average TVOC concentration was 225 μg/m^3 (peak = 3175 μg/m^3). At the FF1 location, during rough extrusion of waste ABS (Figure S4(a)), average particle number concentrations did not exceed 1200 #/cm^3 and peak particle number concentrations were below 4300 #/cm^3. From the APS instrument, GM particle sizes in FF1 were approximately 630 nm during rough and final extrusion and from the OPS instrument, the GM particle size was 317 nm during both rough and final extrusion. During final extrusion of waste ABS (Figure S4(b)), at FF1, average and peak particle number concentrations (P-Trak data) were 3702 #/cm^3 and 9105 #/cm^3, respectively and average and peak TVOC concentrations were 103 μg/m^3 and 874 μg/m^3, respectively. At the FF1 location, only the average particle number concentration measured using a P-Trak was significantly different (*i.e.*, lower) between the rough and final extrusions steps for waste polymers ($p < 0.05$).

Between the NF and FF1 sampling locations during the rough extrusion step, average particle number and TVOC concentrations were not statistically different (all p-values ≥ 0.06), nor were peak particle number and TVOC concentrations statistically different (all p-values ≥ 0.14). During the final extrusion step, none of the average or peak particle number and TVOC concentration measurements were significantly different between the NF and FF1 sampling locations (all p-values ≥ 0.09). While not statistically significant, these small p-values indicate that some differences in particle and TVOC concentrations between sampling locations could exist and should be explored with additional measurements in future studies. Only sufficient PID data was available for statistical comparisons of concentrations at the NF and FF2 sampling locations; there was no difference in average or peak TVOC levels during the rough extrusion task or the final extrusion task (all p-values ≥ 0.15).

Overall, GM particle sizes (APS data) in the NF during extrusion of virgin polymers into filament ranged from 627 nm (HIPS) to 711 nm (PLA). From Supplemental Table S4, from the OPS instrument, GM particle sizes in the NF were approximately 325 nm for all virgin

polymers. Fig. 4 summarizes the particle and TVOC concentrations measured in the NF and FF locations during final extrusion of vPLA and vABS polymers to make filament. During extrusion of vPLA (Fig. 4(a)), in all locations, particle number concentrations (APS, OPS, and P-Trak) did not exceed 100 #/cm^3. During final extrusion of vABS pellets into filament (Fig. 4(b)), average particle concentration in the NF was highest for the P-Trak (4606 #/cm^3), but peak concentration was highest for the APS instrument (53,769 #/cm^3). For vABS, average and peak particle (APS and P-Trak data) and TVOC concentrations were generally lower in the FF locations compared with the NF location. Data for final extrusion of HDPE, LDPE, HIPS, and PP are shown in Supplemental Figure S5. For HDPE, average and peak particle and TVOC concentrations appeared to be lower at the FF locations compared with the NF. For LDPE, all average and peak particle and TVOC metrics generally appeared to be lower at FF1 compared with the NF, although some FF2 values exceeded the NF. During extrusion of HIPS, average and peak particle number concentrations (P-Trak data) appeared lower in the NF compared with FF1, but average and peak TVOC concentrations were higher. Finally, for PP, peak particle number concentrations were highest for the P-Trak instrument and average and peak TVOC levels were higher in the NF compared with FF1. Among all virgin polymers, GM particle sizes at FF1 were 635 nm (vABS) to 663 nm (HDPE) as measured using the APS instrument and 317 nm (vABS) to 326 nm (vPLA) as measured using the OPS instrument. When data from all virgin polymers was combined, only average TVOC concentrations were significantly different between the NF and FF2 sampling locations ($p < 0.05$).

Supplemental Figures S6 to S8 summarize levels of VOCs and metals released during filament making with waste PLA, vPLA, waste ABS, and vABS plastics in the NF, FF1, and FF2 sampling locations, respectively. For the waste PLA and ABS polymers, to increase masses of analytes, a single MCE sample was collected during rough and final extrusions. For waste PLA, low concentrations of eight different VOCs were detected in NF during extrusion; the concentrations of benzene, ethanol, and styrene appeared greater in the NF compared with both FF locations. No metals were quantified at the NF or FF locations during extrusion of waste PLA into filament. For vPLA, five VOCs were quantified in the NF during extrusion (acetone (12.5 μg/m^3), ethanol (707.3 μg/m^3), ethylbenzene (66.7 μg/m^3), toluene (72.7 μg/m^3), and *m,p*-xylene (55.8 μg/m^3)). Concentrations of ethanol appeared greater in the NF compared with the FF locations. For vPLA, low concentrations of Fe and V were quantified in the air at the NF location and only Zn was detected at the FF2 location. During extrusion of waste ABS into filament, low concentrations (no more than 6 μg/m^3) of acetaldehyde, ethanol, n-hexane, styrene, and toluene were measured at the NF location. Additionally, acetone, D-limonene, and *o*-xylene were measured at the FF locations. Only ethanol was detected in all fields and the concentration appeared to be higher in the FF locations compared with the NF. During extrusion of waste ABS into filament, only one of three DNPH samples had measurable formaldehyde (FF1 = 1.9 μg/m^3) at a concentration above background. Levels of caprolactam and BPA were below their respective analytical limits of detection of < 6.7 μg/m^3 and < 0.3 μg/m^3. During extrusion of waste ABS, six different metals were quantified in the NF, three in FF1, and none in FF2 (all < LODs). During extrusion of vABS into filament, low concentrations of four different VOCs were quantified in the air; only acetone and ethanol were detected in the NF and at

least one FF location. For vABS, levels of formaldehyde, caprolactam, and BPA were below their analytical LODs of < 0.2 μg/m^3, < 6.7 μg/m^3, and < 0.9 μg/m^3, respectively.

Supplemental Figures S9 and S10 summarize levels of VOCs and metals released during filament making with virgin HDPE, LDPE, HIPS, and PP at the NF, FF1, and FF2 locations (for HIPS and PP, samples for VOCs were not collected at the FF locations and MCE filter samples were not collected at any location). For HDPE, acetone and ethanol were detected in both the NF and FF1 locations and traces of aluminum (Al), arsenic (As), and Zn were detected, though none of these elements were common to both sampling locations. For LDPE, acetone and ethanol were also detected in both the NF and FF1 locations and a trace of barium was detected at both the NF and FF2 locations. In the NF, during extrusion of HIPS and PP, concentrations of acetone and ethanol were approximately equivalent.

3.3. Contaminant release during FFF 3-D printing with recycled and virgin feedstock filaments

During FFF 3-D printing with recycled filaments, GM particle sizes (APS data) in the NF were 642 nm (rPLA) and 731 nm (rABS). In the FF (APS data), GM particle sizes were approximately 690 nm for both recycled filaments. While printing with vPLA and vABS, the GM particle sizes (APS data) were 722 nm (vPLA) and 741 nm (vABS) in the NF location and 683 nm (vPLA) and 696 nm (vABS) in the FF1 location. During printing with rPLA filament (Fig. 5(a)), in the NF, average and peak particle number concentrations (APS, OPS, and P-Trak) did not exceed 450 #/cm^3. The average TVOC concentration in the NF was 218 μg/m^3 (peak = 4277 μg/m^3). For vPLA (Fig. 5(b)), the average and peak particle number concentrations measured in the NF using an APS were similar to those reported for rPLA. Peak number concentration measured using an FMPS was 708 #/cm^3. The average and peak TVOC concentrations during 3-D printing with rPLA filament appeared higher compared with vPLA filament. During 3-D printing with rABS filament (Fig. 5(c)) and vABS filament (Fig. 5(d)), average and peak particle concentrations in the NF measured using a FMPS instrument were greater compared with a P-Trak instrument, which indicated that most particles were smaller than 20 nm (the lower cut-off of the P-Trak); average and peak TVOC levels in the NF were approximately equivalent between ABS print jobs.

Results of real-time air monitoring during printing with virgin HDPE, LDPE, HIPS, and PP filaments are shown in Supplemental Figure S11. From the APS instrument, GM particle sizes ranged from 616 nm (PP) to 626 nm (HDPE) in the NF and from 644 (PP) to 650 nm (HDPE) at the FF1 location while printing with these virgin filaments. While printing with HDPE filament, average and peak particle number concentrations in the NF measured using an APS (range: 0.5 to 20 μm) were higher than levels measured using a P-Trak (range: 0.02 to 1 μm). For HDPE, since glue was applied to the build platform, the higher APS concentration values could reflect formation of large particles (> 1 μm) from vaporization and condensation of glue to a size that could not be detected by the P-Trak instrument. The extruder nozzle temperature was 235 °C at the start of 3-D printing with HDPE, but it was lowered to 220 °C mid-print. Hence, another possible explanation for the higher concentration counts by the APS instrument compared with the P-Trak is that the higher nozzle temperature, which is known to increase particle concentration (Stabile et al., 2017),

generated more particles that formed large agglomerates detectable by the APS, but not the P-Trak. When the nozzle temperature was decreased mid-print, APS particle counts began to decline (data not shown) indicating fewer agglomerates were formed at the lower nozzle temperature. FFF 3-D printing with LDPE filament generated an average particle concentration of approximately 15 #/cm^3 to 1300 #/cm^3 in the NF. The average TVOC concentration in the NF during printing with LDPE was indistinguishable from background, though a peak concentration of 1520 μg/m^3 was observed. While printing with LDPE, the 3-D printer nozzle clogged, which required a brief (2 min) pause in printing to manually remove the polymer, so these results may not reflect normal print conditions. For HIPS, APS measurements indicated that average particle number concentration in the NF was 60,452 #/cm^3 and peak concentration reached 1.0×10^6 #/cm^3; these values were higher than those measured using a P-Trak. As with HDPE, glue was used to adhere the HIPS print to the build platform so the higher APS concentration values could reflect formation of large particles (> 1 μm) from vaporization and condensation of glue that would not be detected by the P-Trak instrument. Finally, during FFF 3-D printing with PP filament, the average and peak NF particle concentrations were greatest for the P-Trak instrument. When data for all print jobs was combined, based on paired t-tests there was no statistical difference in the average and peak particle number and TVOC concentrations between the NF and FF1 locations (all p-values ≥ 0.14) nor NF and FF2 sampling locations (all p-values ≥ 0.06). Inspection of Fig. 5 and Supplemental Figure 11 indicated that, although not statistically significant, during FFF 3-D printing, there could be differences in particle and TVOC concentrations between sampling locations that should be evaluated with more measurements in future studies.

For rPLA, 10 different VOCs were quantified in air among the NF and FF locations; acetone, benzene, ethanol, and toluene were common among all locations (see Supplemental Figure S12). For vPLA, four aldehydes were quantified in air among all locations. Printing with rABS filament released four different VOCs among all locations (acetone, *D*-limonene, ethanol, and methyl methacrylate) and six aldehydes; formaldehyde (range: 0.5 – 2.5 μg/m^3) and propionaldehyde (range: 0.02 – 0.5 μg/m^3) were common among all sampling locations. During printing with vABS filament, low levels of *D*-limonene were quantified in the NF and FF locations (range: 7.3 – 20.4 μg/m^3). Additionally, six aldehydes were quantified in air, with two common among sampling locations (formaldehyde, range: 0.7 – 2.6 μg/m^3; propionaldehyde, range: 0.05 – 0.6 μg/m^3). Neither caprolactam (< 6.7 μg/m^3) nor BPA (< 0.01 μg/m^3) were detected during FFF 3-D printing with rABS and vABS filaments. Printing with HDPE released acetone and ethanol into the air at all sampling locations. For LDPE, ethanol and formaldehyde were quantified in air during FFF 3-D printing at both the NF and FF1 locations and eight different metals were quantified at trace levels among all sampling locations. Printing with HIPS released acetone and ethanol at both the NF and FF. Finally, with PP filament, only acetone was detected during FFF 3-D printing. Samples were not collected for metals or aldehydes during printing with HIPS and PP polymers.

3.4. Comparison of contaminant releases during filament making and FFF 3-D printing

Fig. 6 compares particle number and TVOC concentrations in the NF during filament making and FFF 3-D printing for all virgin polymers. Paired t-tests indicated that

average and peak particle number concentrations were not significantly different between filament making and FFF 3-D printing (all p-values ≥ 0.20), but average and peak TVOC concentrations were significantly different (p-values < 0.05).

4. Discussion

Distributed recycling of waste polymers at homes and schools has been proposed to create feedstock filament for FFF 3-D printing, though this process can release particles and vapors. To our knowledge, there is no real-world data on contaminant releases during recycling of FFF 3-D printed wastes for incorporation into life cycle assessments. The current study demonstrated that granulation of waste ABS and PLA, two polymers used for 3-D printing (and common household plastics), released measurable concentrations of particles and organic chemicals into a room with an average air exchange rate of 4.5/hr (Fig. 2). Based on paired t-tests, during granulation there was no statistical difference in average and peak particle number and TVOC concentrations between the NF and FF locations. This conclusion is based on a limited number of measurements and should be verified via sampling of more granulation tasks. From the APS and OPS data, particles released during granulation (as well as making filament and FFF 3-D printing of all polymers) had submicron size, which was sufficiently small to deposit in the gas exchange region of the lung where clearance is slow (ICRP, 1994). In the current study, the granulator was only tested in one configuration; changes in the input energy, cutting elements (orientation, sharpness, configuration) could also change particle number and size distributions, which would in turn influence dosimetry and should be explored in future studies. Vapor releases included low concentrations of acetaldehyde, acetone, benzene, toluene, *m,p*-xylene, and *o*-xylene during granulation of waste PLA polymer and acetaldehyde and acetone during granulation of waste ABS polymer (Supplemental Figure S3). Benzene and acetaldehyde are respiratory irritants and classified by NIOSH as potential occupational carcinogens (NIOSH, 2005). Acetone, toluene, and xylenes are mucus membrane irritants and central nervous system depressants (NIOSH, 2005).

Byrley et al. evaluated particle emissions during extrusion of virgin ABS and two virgin PLA materials to make FFF 3-D printer filaments in a laboratory test chamber (Byrley et al., 2019). Like the virgin polymers used in our study, their polymers were not previously extruded on a FFF 3-D printer but contained white colorants. In their study, particle concentrations were greater for ABS compared with PLA. In our study, filament making by extrusion was performed in a room with AER of 9.3/hr and average particle concentrations (APS and P-Trak data) were greater for rABS than rPLA, although peak concentrations tended to be greater for the latter (Fig. 3 and Figure S4). For the vABS and vPLA materials, our APS and P-Trak average and peak number concentrations recorded during the filament making task were consistent with Byrley et al. (see Fig. 4).

For waste PLA, acetone, benzene, ethanol, ethylbenzene, n-hexane, methyl methacrylate, α-pinene, styrene, toluene, *m,p*-xylene, and *o*-xylene were detected among all sampling locations during filament making. For waste ABS, eight different organic gasses (acetaldehyde, acetone, ethanol, n-hexane, D-limonene, styrene, toluene, and *o*-xylene) were detected in the NF and FF locations during filament making. During extrusion of vPLA

into filament, acetone, benzene, ethanol, ethylbenzene, styrene, toluene, and *m,p*-xylene were quantified in air among all fields and during extrusion of vABS low concentrations of acetaldehyde, acetone, benzene, and ethanol were quantified in air (Supplemental Figures S6 to S8). As noted above, acetone, benzene, toluene, and xylene are associated with adverse health effects. Ethyl-benzene and methyl methacrylate are mucus membrane and respiratory irritants; formaldehyde is a respiratory irritant and classified by NIOSH as a potential occupational carcinogen; and styrene is a respiratory irritant and asthmagen (Nett et al., 2017; NIOSH, 2005). In the presence of ozone, α-pinene reacts to form carbonyl compounds such as formaldehyde (Jackson et al., 2017) and D-limonene forms multiple carbonyl compounds (Ham et al., 2016). Exposure to carbonyl compounds are associated with occupational asthma (Jarvis et al., 2005). Byrley et al. reported that extrusion of a virgin ABS material to make filament released styrene. We also observed the release of styrene during extrusion of waste ABS polymer into filament (but not during extrusion of vABS). Byrley et al. evaluated VOC releases during extrusion of PLA pellets into FFF 3-D printer filament and observed the release of acetone, benzene, and toluene; extrusion of pulverized PLA released the same VOCs as well as styrene. In the current study, during extrusion of PLA, the same four VOCs as reported by Byrley et al., as well as ethanol, ethylbenzene, n-hexane, methyl methacrylate, *α*-pinene, *m,p*-xylene, and *o*-xylene were released into air.

Byrley et al. (2019) noted that the manufacturer's recommended temperature for extrusion of a polymer into filament was lower than their recommended temperature for FFF 3-D printing with that same polymer (see Supplemental Figure S13). In their study, measured particle number-based concentrations and emission rates for extrusion of ABS and PLA polymers were reported to be similar compared with literature values for FFF 3-D printing with the same types of filaments. In our study, for the virgin polymer materials, average and peak particle number concentrations were not statistically different between the filament making and 3-D printing tasks; however, the average and peak TVOC concentrations were significantly different. The general similarity of average particle concentrations between the filament making and FFF 3-D printing tasks was somewhat surprising given that several prior studies have reported that particle (and/or TVOC) levels increased as printer nozzle temperature increased (Davis et al., 2019; Deng et al., 2016; Ding et al., 2019; Gu et al., 2019; Jeon et al., 2020; Mendes et al., 2017; Poikkimäki et al., 2019; Stabile et al., 2017). The exact reason why particle levels were similar during filament making and FFF 3-D printing with the same filament is unclear. Byrley et al. postulated that, although at a lower temperature, there was greater contact area between polymer and the screw and extrusion nozzle inside the extruder machine compared with a higher temperature, but smaller area of contact, within the FFF 3-D printer nozzle, which could result in releases of particles being comparable (Byrley et al., 2019). Another factor that could explain or contribute to the similarity between tasks is the relative time spent in contact with heated surfaces in these machines. The feed rates of polymer through the extruder screw feeder were slower compared with an FFF 3-D printer nozzle; it is possible that the longer polymer residence time in the extruder compared with the nozzle could compensate for differences in temperature, thereby yielding similar particle emissions. The reason why TVOC levels were higher during filament making compared with FFF 3-D printing is not known positively.

Each time a polymer is heated its mechanical properties are degraded (Cruz-Sanchez et al., 2017). Hence, it is possible that TVOC concentrations were significantly higher during filament extrusion compared with FFF 3-D printing because of differences in changes in the mechanical and thermal properties of the polymer from the unique thermal profiles of these tasks. For example, in one study of PLA, over five extrusion and print cycles, extruded filament exhibited considerable reductions in tensile strength, tensile strength at break, tensile strain and nominal strain at break whereas printed parts exhibited a slight reduction in these properties (Cruz Sanchez et al., 2017). In a study of ABS polymer, Mohammed et al. (2019) reported that compared with vABS, filaments made from rABS exhibited a decrease in the polymer melt flow index, which indicated a decrease in polymer molecular weight, and therefore thermal stability. It has been reported that for HDPE polymer, TVOC levels decreased with repeated extrusion cycles while the polymer became more brittle and had decreased thermal properties. Hence, it is possible that during its first heating (extrusion) as a polymer undergoes changes in mechanical and thermal properties it releases the highest amount of organic vapors and during subsequent heating (FFF 3-D printing) vapor release levels decline as the changes in polymer properties continue and the amount of volatiles is depleted further. To confirm this possible explanation, future studies are needed in which the mechanical and thermal properties of polymers are measured in conjunction with emissions during repeated extrusions into filament and FFF 3-D printing.

The results reported by Byrley et al. and the current study indicated that extrusion of waste and virgin polymers to make feedstock filament for FFF 3-D printing as part of a distributed recycling process released particles and gas-phase mucous membrane irritants, respiratory irritants, asthmagens, potential occupational carcinogens, and central nervous system depressants into indoor air. There are no particle number-based occupational exposure limits (OELs) to which our results can be compared. Generally speaking, measured levels of VOCs and elements were well below OELs (NIOSH, 2005); however, these limits are for individual substances and not complex mixtures, which could have additive or synergistic effects on the body. Additionally, typical AER in U.S. homes and newly constructed classrooms are 0.45/hr and 2.0/hr, respectively (Batterman et al., 2017; EPA, 2018) which are much lower than the AER of 9.3/hr in the teaching laboratory. Hence, less air exchange in homes and classrooms could result in higher particle number and VOC concentrations than reported here as general ventilation in these types of settings can be insufficient to remove contaminants released from FFF 3-D printers (Viitanen et al., 2021). As noted previously, we targeted specific chemicals of health concern with our vapor sampling strategy; however, more chemicals than we measured were likely emitted (see, for example, Davis et al., 2019 or Zhu et al., 2020) and future life cycle assessments might want to include other chemicals of health relevance. Further, susceptible bystanders such as children, the elderly, and persons with compromised immune systems may occupy spaces where distributed recycling, polymer extrusion, and FFF 3-D printing are performed and OELs might not protect these vulnerable populations. In the current study, during granulation, extrusion, and FFF 3-D printing tasks most particle number and TVOC metrics did not differ between the NF and FF locations, which indicated the potential for exposures to users and bystanders alike. Our results were in contrast to prior studies that reported levels of contaminants were higher in the NF compared with the FF during additive manufacturing

processes (Bau et al., 2020; Bharti and Singh, 2017; Lewinski et al., 2019) or higher in the FF compared with the NF (Chan et al., 2020; Zhou et al., 2015), but consistent with a report of no differences in contaminant levels between fields (Chan et al., 2020). NF and FF contaminant concentrations can depend on several factors such as contaminant type and form and air flow patterns in the room. As such, it is prudent to control contaminant releases at the source using local exhaust ventilation when distributed recycling is performed in offices, homes, schools, libraries, or any other space with insufficient ventilation.

FFF 3-D printing holds great promise for distributed recycling and has circular economy potential through production of value-added parts from waste via personal fabrication (Baechler et al., 2013; Hunt et al., 2015; Kreiger et al., 2014; Peeters et al., 2019). FFF 3-D printing offers many potential societal benefits (Huang et al., 2013); however, if not used with adequate controls, this technology can release hazardous particles and vapors into air. Peeters et al. explored barriers to distributed recycling of FFF 3-D printer waste and reported that meeting consumer demands for high quality printed parts was among the primary barriers to adoption, whereas health and safety considerations had little driving power in adoption (Peeters et al., 2019). Polymeric materials undergo thermo-mechanical degradation via high shear forces and high temperatures during reprocessing, which causes chain scissions and chemical reactions that result in changes in crystallinity and thermal stability that might affect part quality (Cruz Sanchez et al., 2017; Zhao et al., 2018). Such changes to polymers can present challenges for the use of recycled filament during FFF 3-D printing (Anderson, 2017). For example, one study reported that rPLA could only be reprocessed for two FFF 3-D printing/recycling cycles as it was no longer printable for a third cycle (Zhao et al., 2018). In the current study, we recycled PLA and ABS waste plastics into filament once and successfully used both polymers to FFF 3-D print parts (see Figure S1) while monitoring emissions. Understanding is limited on how changes in polymer properties as a result of recycling impacts the release of particles and vapors into indoor air during granulation, extrusion, and 3-D printing and should be evaluated as part of future studies to demonstrate their circular economy potential.

5. Conclusions

These distributed recycling processes released particles and potentially hazardous vapors (mucous membrane irritants, respiratory irritants, asthmagens, potential occupational carcinogens, and central nervous system depressants) into indoor air that could be breathed in by room occupants. From the real-time measurements, ABS, PLA, and HIPS polymers were associated with the greatest particle number concentration (P-Trak data) and TVOC concentration measurements during granulation, extrusion, and FFF 3-D printing. These results provide valuable data for future life cycle assessments of FFF 3-D printing sustainability in the context of distributed recycling and circular economy potential, which should account for human exposures and potential health risks (Bours et al., 2017).

Supplementary Material

Refer to Web version on PubMed Central for supplementary material.

Acknowledgements

The authors thank D. Hammond and D. Thompson at NIOSH for critical review of this manuscript prior to submission to the journal and A. Ranpara and D. Burns at NIOSH for analysis of canister samples. The findings and conclusions in this report are those of the authors and do not necessarily represent the official position of the National Institute for Occupational Safety and Health, Centers for Disease Control and Prevention. This work was supported by the U.S. Consumer Product Safety Commission under Interagency Agreement 61320619H0100 and NIOSH intramural research funds. This work has not been reviewed or approved by and does not necessarily represent the views of, the Commission. Certain commercial equipment, instruments, or materials are identified in this paper in order to specify the experimental procedure adequately. Such identification is not intended to imply recommendation or endorsement by the Consumer Product Safety Commission, nor is it intended to imply that the materials or equipment identified are necessarily the best available for the purpose.

References

Anderson I, 2017. Mechanical properties of specimens 3D printed with virgin and recycled polylactic acid. 3D Print Addit. Manuf 4 (2), 110–115.

ASTM, 2017. E741–11: standard test method for determining air change in a single zone by means of a tracer gas dilution. ASTM, West Conshohocken, PA.

Baechler C, Devuono M, Pearce JM, 2013. Distributed recycling of waste polymer into RepRap feedstock. Rapid Proto. J 19 (2), 118–125.

Batterman S, Su FC, Wald A, Watkins F, Godwin C, Thun G, 2017. Ventilation rates in recently constructed U.S. school classrooms. Indoor Air 27 (5), 880–890. [PubMed: 28370427]

Bau S, Rousset D, Payet R, Keller FX, 2020. Characterizing particle emissions from a direct energy deposition additive manufacturing process and associated occupational exposure to airborne particles. J. Occup. Environ. Hyg 17 (2–3), 59–72. [PubMed: 31829796]

Bharti N, Singh S, 2017. Three-dimensional (3D) printers in libraries: perspective and preliminary safety analysis. J. Chem. Ed 94 (7), 879–885.

Bours J, Adzima B, Gladwin S, Cabral J, Mau S, 2017. Addressing hazardous implications of additive manufacturing: complementing life cycle assessment with a framework for evaluating direct human health and environmental impacts. J. Indust. Ecol 21 (S1), S25–S36.

Byrley P, George BJ, Boyes WK, Rogers K, 2019. Particle emissions from fused deposition modeling 3D printers: evaluation and meta-analysis. Sci. Total Environ 655, 395–407. [PubMed: 30471608]

Chan FL, Hon CY, Tarlo SM, Rajaram N, House R, 2020. Emissions and health risks from the use of 3D printers in an occupational setting. J. Toxicol. Environ. Health A 83 (7), 279–287. [PubMed: 32316869]

Cruz Sanchez FA, Boudaoud H, Hoppe S, Camargo M, 2017. Polymer recycling in an open-source additive manufacturing context: mechanical issues. Addit. Manuf 17, 87–105.

Cruz Sanchez FA, Boudaoud H, Camargo M, Pearce JM, 2020. Plastic recycling in additive manufacturing: a systematic literature review and opportunities for the circular economy. J. Cleaner Prod 264. Article Number 121602.

Davis AY, Zhang Q, Wong JPS, Weber RJ, Black MS, 2019. Characterization of volatile organic compound emissions from consumer level material extrusion 3D printers. Build Environ. 160. Article Number 106209.

Deng Y, Cao SJ, Chen A, Guo Y, 2016. The impact of manufacturing parameters on submicron particle emissions from a desktop 3D printer in the perspective of emission reduction. Build Environ. 104, 311–319.

Ding S, Ng BF, Shang X, Liu H, Lu X, Wan MP, 2019. The characteristics and formation mechanisms of emissions from thermal decomposition of 3D printer polymer filaments. Sci. Total Environ 692, 984–994. [PubMed: 31540002]

Du Preez S, Johnson A, LeBouf RF, Linde SJL, Stefaniak AB, Plessis Du, 2018. Exposures during industrial 3-D printing and post-processing tasks. Rapid Proto. J 24 (5), 865–871.

EPA, 1999. Method TO-11A: Determination of Formaldehyde in Ambient Air Using Adsorbent Cartridge Followed By High Performance Liquid Chromatography (HPLC) [Active Sampling Methodology]. U.S. Environmental Protection Agency, Cincinnati, OH.

EPA, 2018. Update For Chapter 19 of the Exposure Factors Handbook. Building Characteristics. U.S. Environmental Protection Agency, Washington, D.C.

Gu J, Wensing M, Uhde E, Salthammer T, 2019. Characterization of particulate and gaseous pollutants emitted during operation of a desktop 3D printer. Environ. Int 123, 476–485. [PubMed: 30622073]

Ham JE, Harrison JC, Jackson SR, Wells JR, 2016. Limonene ozonolysis in the presence of nitric oxide: gas-phase reaction products and yields. Atmos. Environ 132, 300–308.

Huang SH, Liu P, Mokasdar A, Hou L, 2013. Additive manufacturing and its societal impact: a literature review. Int. J. Adv. Manuf. Technol 67 (5–8), 1191–1203.

Hunt EJ, Zhang C, Anzalone N, Pearce JM, 2015. Polymer recycling codes for distributed manufacturing with 3-D printers. Resour. Conserv. Recycl 97, 24–30.

ICRP, 1994. International Commission on Radiological Protection. Publication 66: Human respiratory tract model for radiological protection Pergamon, Oxford, UK.

ISO/ASTM, 2015. 52900: Additive Manufacturing — General principles — Terminology. ISO, Geneva, Switzerland.

Jackson SR, Harrison JC, Ham JE, Wells JR, 2017. A chamber study of alkyl nitrate production formed by terpene ozonolysis in the presence of NO and alkanes. Atmos. Environ 171, 132–148.

Jarvis J, Seed MJ, Elton RA, Sawyer L, Agius RM, 2005. Relationship between chemical structure and the occupational asthma hazard of low molecular weight organic compounds. Occup. Environ. Med 62 (4), 243–250. [PubMed: 15778257]

Jeon H, Park J, Kim S, Park K, Yoon C, 2020. Effect of nozzle temperature on the emission rate of ultrafine particles during 3D printing. Indoor Air 30 (2), 306–314. [PubMed: 31743481]

Kreiger MA, Mulder ML, Glover AG, Pearce JM, 2014. Life cycle analysis of distributed recycling of post-consumer high density polyethylene for 3-D printing filament. J. Cleaner. Prod 70, 90–96.

Lewinski NA, Secondo LE, Ferri JK, 2019. On-site three-dimensional printer aerosol hazard assessment: pilot study of a portable in vitro exposure cassette. Proc. Safety. Prog 38 (3). Article Number e12030.

Mendes L, Kangas A, Kukko K, Mølgaard B, Säämänen A, Kanerva T, Flores Ituarte I, Huhtiniemi M, Stockmann-Juvala H, Partanen J, Hämeri K, Eleftheriadis K, Viitanen AK, 2017. Characterization of emissions from a desktop 3D printer. J. Indust. Ecol 21, S94–S106.

Mikula K, Skrzypczak D, Izydorczyk G, Warchoł J, Moustakas K, Chojnacka K, Witek-Krowiak A, 2021. 3D printing filament as a second life of waste plastics—A review. Environ. Sci. Poll. Res 28, 12321–12333.

Mohammed MI, Wilson D, Gomez-Kervin E, Tang B, Wang J, 2019. Investigation of closed-loop manufacturing with acrylonitrile butadiene styrene over multiple generations using additive manufacturing. ACS Sustain Chem. Eng 7 (16), 13955–13969.

Nett RJ, Cox-Ganser JM, Hubbs AF, Ruder AM, Cummings KJ, Huang YT, Kreiss K, 2017. Non-malignant respiratory disease among workers in industries using styrene-A review of the evidence. Am. J. Ind. Med 60 (2), 163–180. [PubMed: 28079275]

NIOSH, 2003. Method 7303: Elements by ICP (Hot Block/HCl/HNO3 Digestion), NIOSH Manual of Analytical Methods, 4th Edition. U.S. Department of Health and Human Services, Public Health Service, Centers for Disease Control and Prevention, National Institute for Occupational Safety and Health, Cincinnati, OH.

NIOSH, 2005. Pocket Guide to Chemical Hazards. http://www.cdc.gov/niosh/npg/default.html. (Accessed April 20, 2021.

NIOSH, 2016. Method 2016: formaldehyde, issue 3. In: Ashley K, O'Connor PF (Eds.), NIOSH Manual of Analytical Methods, 5th Edition. U.S. Department of Health and Human Services, Public Health Service, Centers for Disease Control and PreventionNational Institute for Occupational Safety and Health, Cincinnati, OH.

NIOSH, 2018. Method 3900: volatile Organic Compounds, C1 to C10, Canister Method. In: Ashley K, O'Connor PF (Eds.), NIOSH Manual of Analytical Methods, 5th Edition. U.S. Department of Health and Human Services, Public Health Service, Centers for Disease Control and Prevention, National Institute for Occupational Safety and Health, Cincinnati, OH.

OSHA, 1988. Method PV2012: caprolactam. OSHA Salt Lake Technical Center, Salt Lake City, UT.

OSHA, 2013. Method 1018: bisphenol A and Diglycidyl Ether of Bisphenol A. https://www.osha.gov/laws-regs/regulations/standardnumber/1910/1910.1450. (Accessed January 29, 2020.

Pakkanen J, Manfredi D, Minetola P, Iuliano L, 2017. About the use of recycled or biodegradable filaments for sustainability of 3D printing: state of the art and research opportunities. Smart Innov. Syst. Tech 68, 776–785.

Peeters B, Kiratli N, Semeijn J, 2019. A barrier analysis for distributed recycling of 3D printing waste: taking the maker movement perspective. J. Cleaner Prod 241, Article Number 118313.

Poikkimäki M, Koljonen V, Leskinen N, Närhi M, Kangasniemi O, Kausiala O, Dal Maso M, 2019. Nanocluster aerosol emissions of a 3D printer. Environ. Sci. Technol 53 (23), 13618–13628. [PubMed: 31697477]

Song R, Clemon L, Telenko C, 2019. Uncertainty and variability of energy and material use by fused deposition modeling printers in makerspaces. J. Indust. Ecol 23 (3), 699–708.

Song R, Telenko C, 2016. Material waste of commercial FDM printers under realistic conditions, Solid Freeform Fabrication. 2016: Proc. of the 27th Ann. Int. Solid Freeform Fabrication Symposium - An Additive Manufacturing Conference, SFF 2016 1217–1229.

Song R, Telenko C, 2017. Material and energy loss due to human and machine error in commercial FDM printers. J. Cleaner Prod 148, 895–904.

Stabile L, Scungio M, Buonanno G, Arpino F, Ficco G, 2017. Airborne particle emission of a commercial 3D printer: the effect of filament material and printing temperature. Indoor Air 27 (2), 398–408. [PubMed: 27219830]

Stefaniak A, Bowers L, Cottrell G, Erdem E, Knepp A, Martin S, Pretty J, Duling M, Arnold E, Wilson Z, Krider B, LeBouf R, Virji M, Sirinterlikci A, 2021c. Use of 3-dimensional printers in educational settings: the need for awareness of the effects of printer temperature and filament type on contaminant releases. ACS Chem. Health Saf 10.1021/acs.chas.1c00041 (revised).

Stefaniak A, Bowers L, Martin S, Hammond D, Ham J, Wells J, Fortner A, Knepp A, du Preez S, Pretty JR, Roberts JL, du Plessis J, Duling MG, Virji MA, 2021a. Large format additive manufacturing and machining using high melt temperature polymers. Part II: characterization of particulate and gases. ACS Chem. Health Saf 10.1021/acs.chas.0c00129.

Stefaniak AB, Du Preez S, Du Plessis JL, 2021b. Additive manufacturing for occupational hygiene: a comprehensive review of processes, emissions, & exposures. J. Toxicol. Environ. Health B Crit. Rev 24, 173–222.

Stefaniak AB, Johnson AR, du Preez S, Hammond DR, Wells JR, Ham JE, LeBouf RF, Menchaca KW, Martin SB Jr., Duling MG, Bowers LN, Knepp AK, Su FC, de Beer DJ, du Plessis JL, 2019. Evaluation of emissions and exposures at workplaces using desktop 3-dimensional printers. J. Chem. Health Saf 26 (2), 19–30. [PubMed: 31798757]

Suárez L, Domínguez M, 2020. Sustainability and environmental impact of fused deposition modelling (FDM) technologies. Int. J. Adv. Manuf. Technol 106 (3–4), 1267–1279.

Thomas D, 2016. Costs, benefits, and adoption of additive manufacturing: a supply chain perspective. Int. J. Adv. Manuf. Technol 85 (5–8), 1857–1876. [PubMed: 28747809]

Viitanen AK, Kallonen K, Kukko K, Kanerva T, Saukko E, Hussein T, Hämeri K, Säämänen A, 2021. Technical control of nanoparticle emissions from desktop 3D printing. Indoor Air 31 (4), 1061–1071. [PubMed: 33647162]

Wu H, Fahy WP, Kim S, Kim H, Zhao N, Pilato L, Kafi A, Bateman S, Koo JH, 2020. Recent developments in polymers/polymer nanocomposites for additive manufacturing. Prog. Mat. Sci 111, 100638.

Zhao P, Rao C, Gu F, Sharmin N, Fu J, 2018. Close-looped recycling of polylactic acid used in 3D printing: an experimental investigation and life cycle assessment. J. Cleaner Prod 197, 1046–1055.

Zhong S, Pearce JM, 2018. Tightening the loop on the circular economy: coupled distributed recycling and manufacturing with recyclebot and RepRap 3-D printing. Resour. Conserv. Recycl 128, 48–58.

Zhou Y, Kong X, Chen A, Cao S, 2015. Investigation of ultrafine particle emissions of desktop 3D printers in the clean room. Procedia. Eng 121, 506–512.

Zhu Q, Yao Q, Liu J, Sun J, Wang Q, 2020. Emissions from the fused filament fabrication 3D printing with lignocellulose/polylactic acid filament. Bioresources 15, 7560–7572.

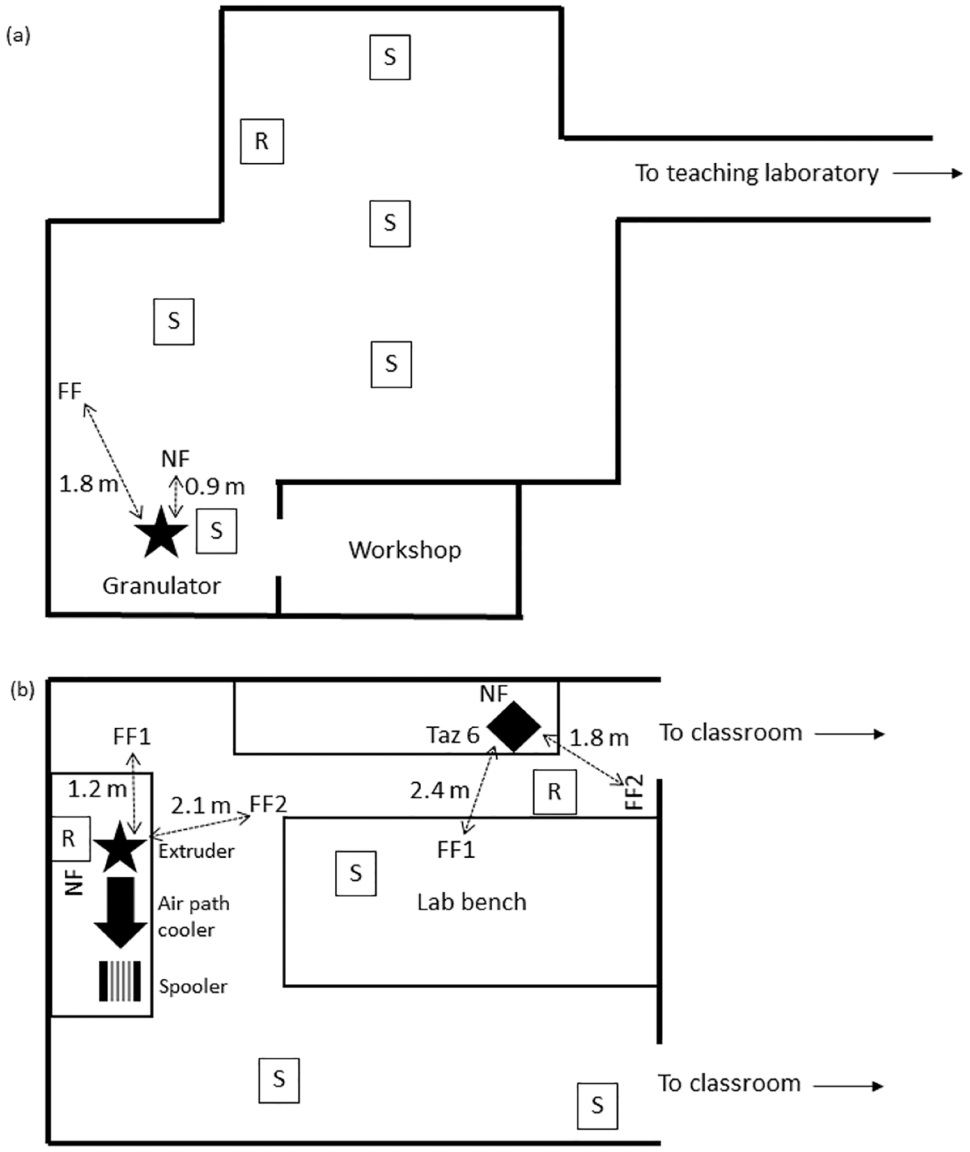

Fig. 1.

Room layouts and sampling locations for (a) granulation of waste polymer (608 m^3 engineering laboratory), (b) extrusion of waste and virgin polymer into feedstock filament and FFF 3-D printing with all filaments (278 m^3 teaching laboratory). NF = near field sampling location, FF/FF1/FF2 = far field sampling locations, *S* = ceiling ventilation supply air vent, *R* = ceiling ventilation return air vent. Drawings not to scale.

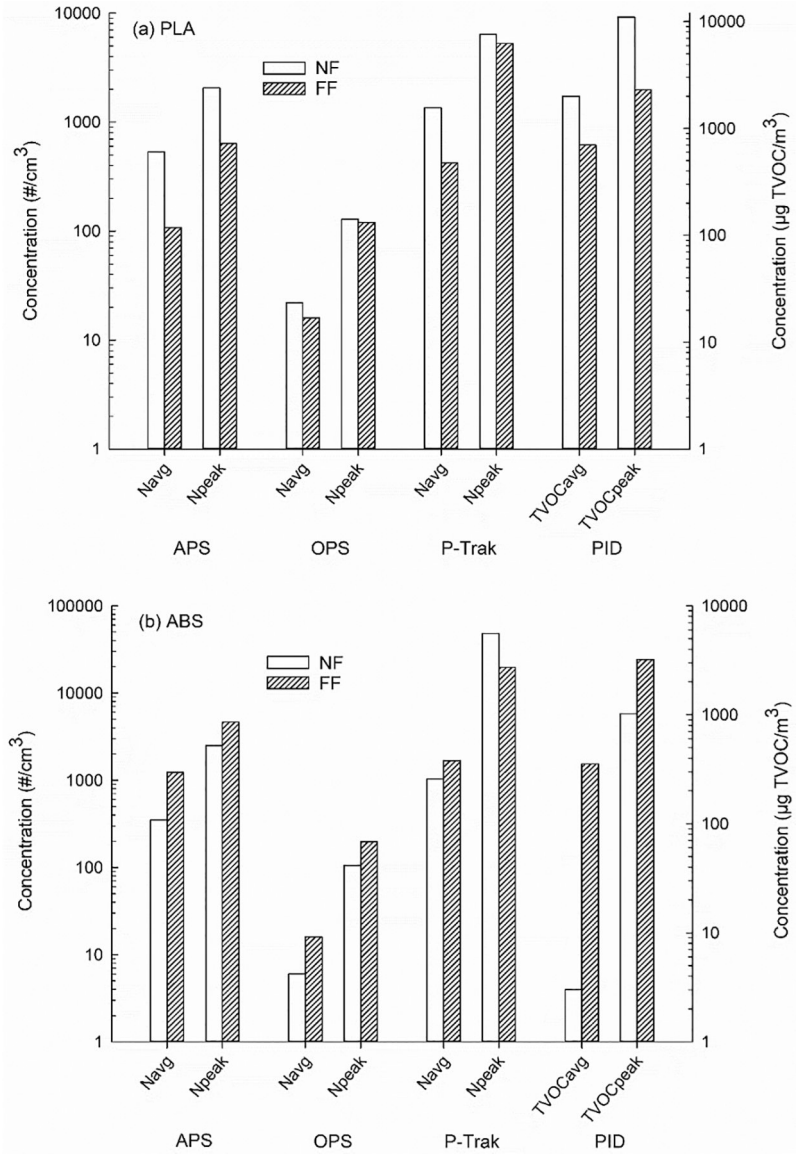

Fig. 2.

Real-time average and peak particle number and total volatile organic compound (TVOC) concentrations in the near field (NF) and far field (FF) during granulation of waste polymers: (a) polylactic acid (PLA), (b) acrylonitrile butadiene styrene (ABS). APS = aerodynamic particle sizer, OPS = optical particle sizer, P-Trak = condensation particle counter, PID = TVOC photoionization detector.

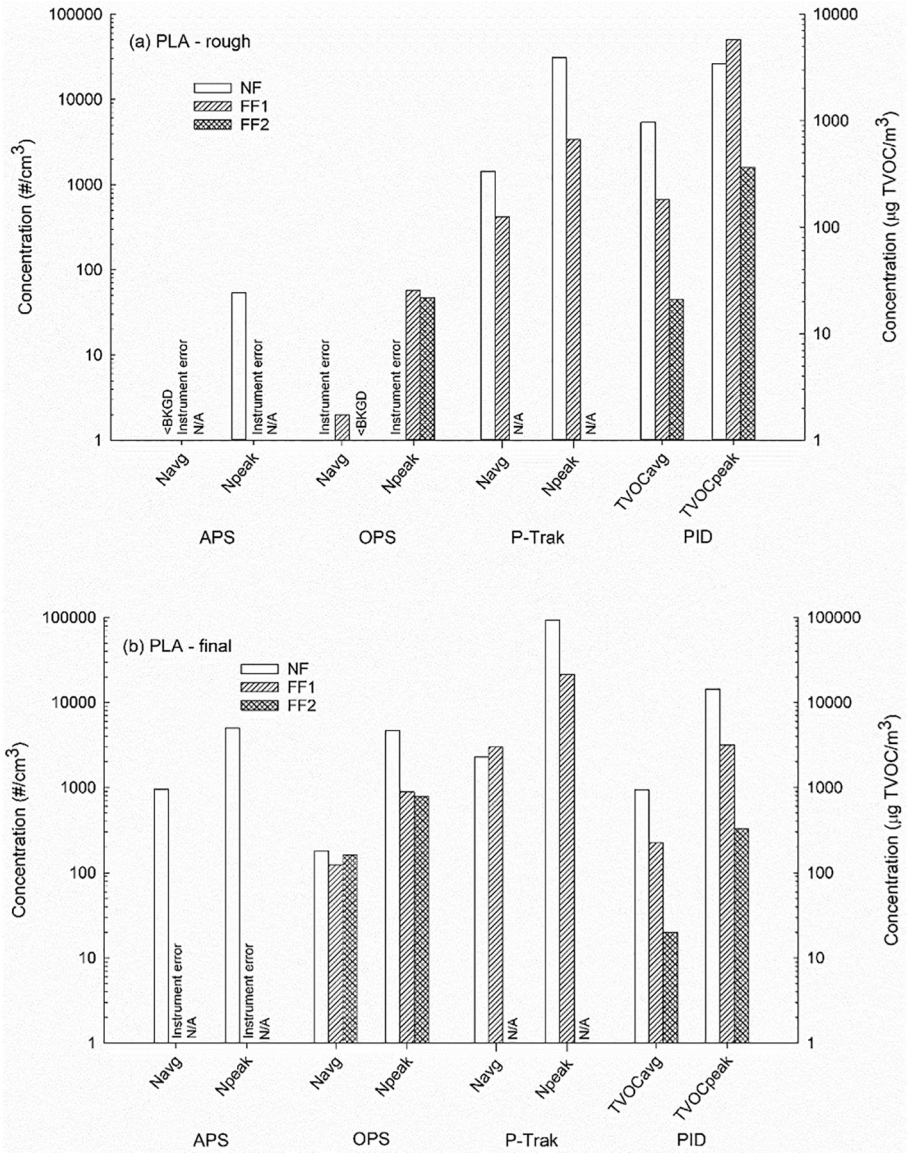

Fig. 3.

Average and peak particle number and total volatile organic compound (TVOC) concentrations in the near field (NF), far field 1 (FF1), and far field 2 (FF2) sampling locations during extrusion of waste polylactic acid (PLA) plastic into FFF 3-D printer filament: (a) rough extrusion, (b) final extrusion. APS = aerodynamic particle sizer, OPS = optical particle sizer, P-Trak = condensation particle counter, PID = TVOC photoionization detector. N/*A* = no sample collected.

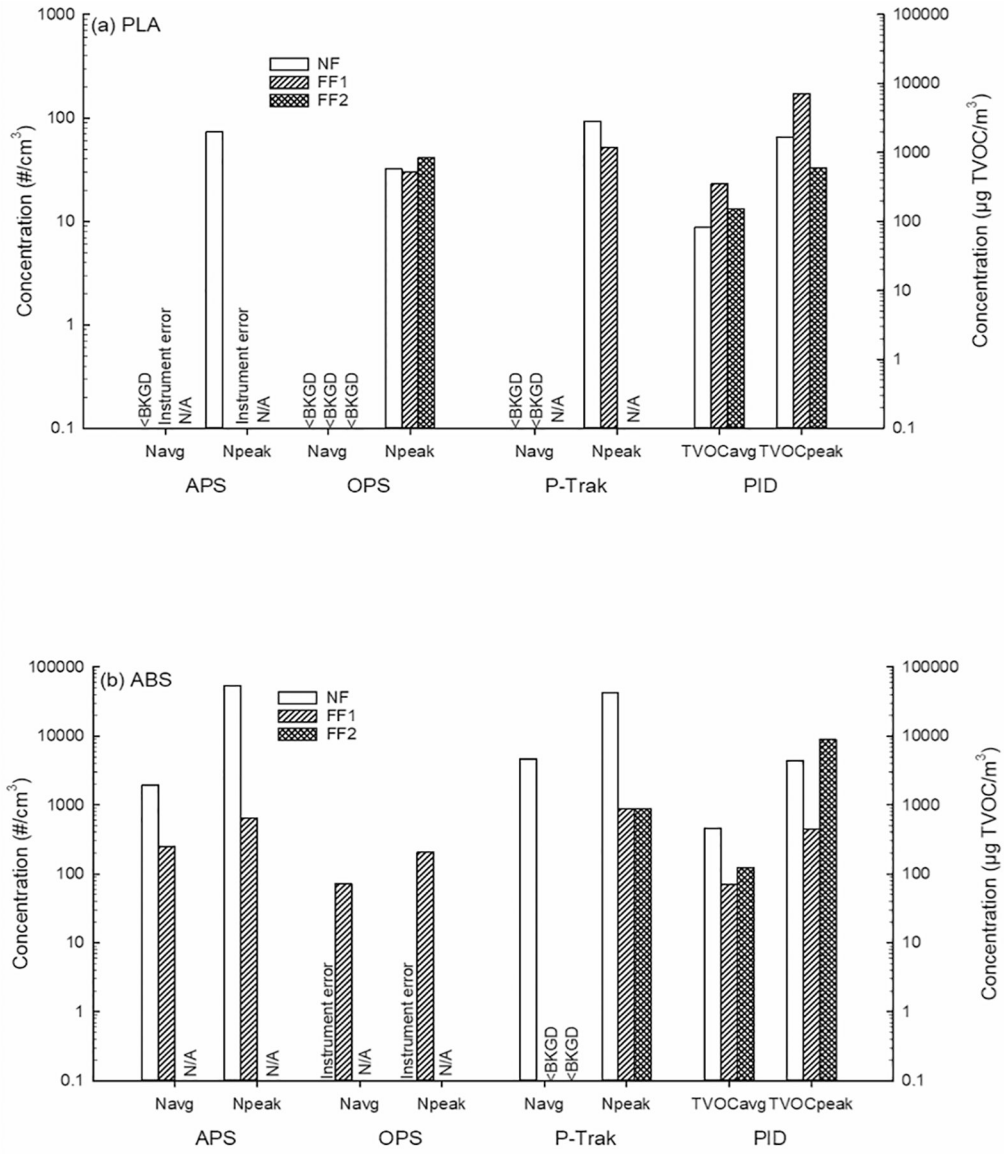

Fig. 4.

Average and peak particle number and total volatile organic compound (TVOC) concentrations in the near field (NF), far field 1 (FF1), and far field 2 (FF2) sampling locations during final extrusion of virgin polymers into FFF 3-D printer filaments: (a) polylactic acid (PLA) and (b) acrylonitrile butadiene styrene (ABS). APS = aerodynamic particle sizer, OPS = optical particle sizer, P-Trak = condensation particle counter, PID = TVOC photoionization detector. N/*A* = no sample collected.

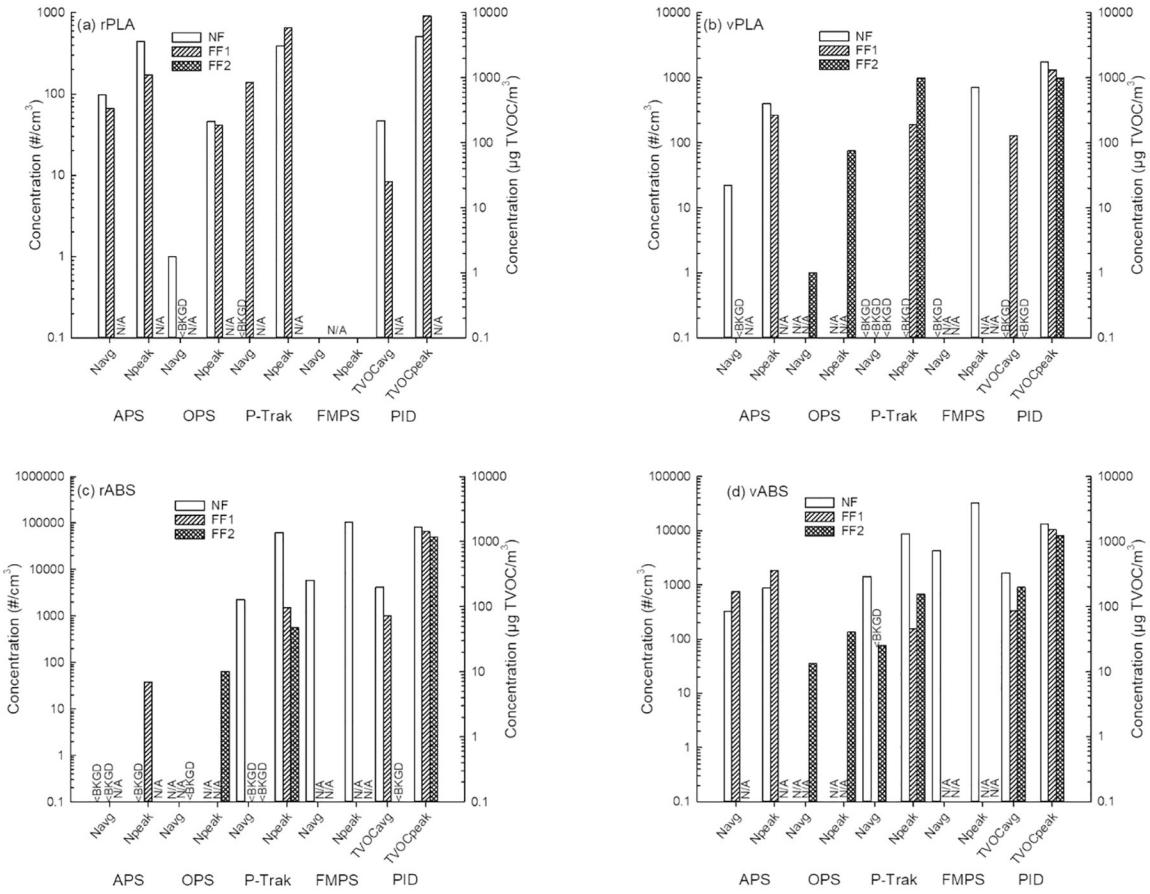

Fig. 5.

Average and peak particle number and total volatile organic compound (TVOC) concentrations in the near field (NF), far field 1 (FF1), and far field 2 (FF2) sampling locations during FFF 3-D printing with various filaments: (a) recycled polylactic acid (rPLA), (b) virgin PLA, (c) recycled acrylonitrile butadiene styrene (rABS), and (d) virgin ABS. APS = aerodynamic particle sizer, OPS = optical particle sizer, P-Trak = condensation particle counter, FMPS = fast mobility particle sizer, PID = TVOC photoionization detector. N/*A* = no sample collected.

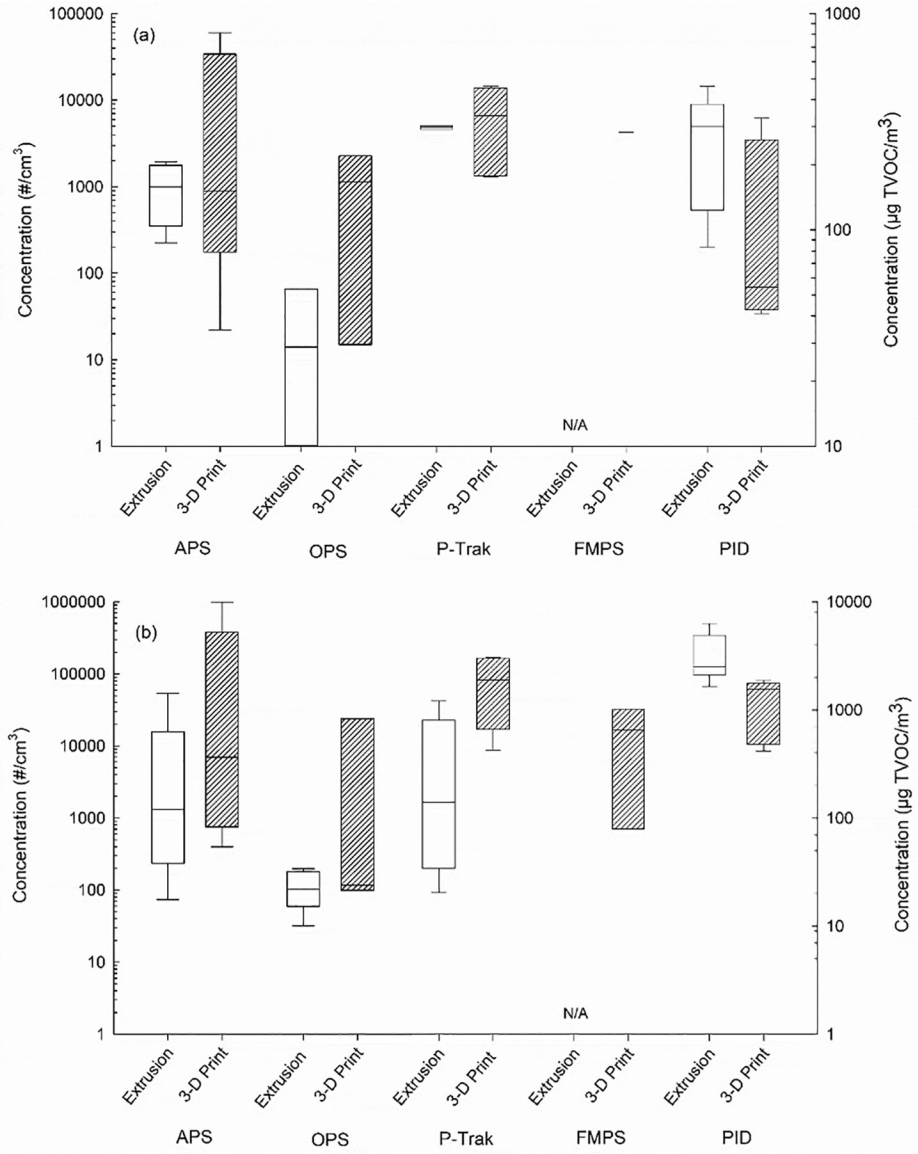

Fig. 6.

Particle number and TVOC concentrations in the NF during extrusion of virgin polymer materials into filament and FFF 3-D printing with these filaments: (a) average concentrations, (b) peak concentrations. Top and bottom whiskers represent the 90th and 10th percentiles, respectively. The upper boundary of the box is the 75th percentile, the line in the box is the 50th percentile (median), and the lower boundary of the box is the 25th percentile. APS = aerodynamic particle sizer, OPS = optical particle sizer, P-Trak = condensation particle counter, FMPS = fast mobility particle sizer, PID = TVOC photoionization detector. N/*A* = no sample collected.